Pergamon

Tetrahedron Vol. 50, No. 47, pp. 13377-13394, 1994

0040-4020/94 $7.00+0.00

0040-4020(94)00870-1

Combined NMR Spectroscopy and Molecular Mechanics Studies of OH-Depleted Calix[4]arenes: On the Influence of OH Groups on the Relative Stability of Calix[4]arene Conformers

Takaaki Harada, Fumio Ohseto and Seiji Shinkai*

Chemirecognics Project, ERATO, Research Development Corporation of Japan,
Aikawa 2432-3, Kurume, Fukuoka 830, Japan

Abstract: The effects of OH groups on the relative stabilities and the structures of four conformers of OH-depleted calix[4]arenes are discussed on the basis of a computational method using molecular mechanics (MM3(92)) calculations. The results are compared with various NMR spectroscopic experiments. From these studies, it is found that the calix[4]arene framework with no OH group in the lower rim (tetra-OH-depleted calix[4]arenes: **4a** and **4b**) favors a cone conformation with C_4 symmetry and the changes in the relative stabilities in calix[4]arenes with OH-groups are due to the formation of stable hydrogen bonds and/or the relaxation of the steric crowding around OH-substituents in a lower rim site. NMR studies suggest that mono-OH-depleted calix[4]arene **1b** forms intra- and intermolecular hydrogen bonds among phenolic OH groups, while di- and tri-OH-depleted calix[4]arenes (**2b** and **3b**) scarcely form it. They also show that the ring inversion barriers of calix[4]arenes increase with the number of OH groups in 25, 26, 27 or 28-position.

Introduction

Computational studies of conformational isomerism in calix[n]arenes and their analogs have been of much recent concern.[1-6] Among them, a calix[4]arene family draws particular interest because calix[4]arenes consist of a 16-membered ring but generate only four significant conformers, cone, partial cone, 1,2-alternate and 1,3-alternate.[7,8] This situation makes the initial conditions of the computational analysis much simpler. The limitation in the conformational freedom has been attributed to the rigid metacyclophane framework.[7-9] In 1990, Grootenhuis *et al.*[3] reported extensive computational studies on calix[4]arenes using several force fields. They succeeded in the computational elucidation of several characteristics of calix[4]arenes. A few but essential observations, however, remained unexplainable. In the case of calix[4]arene-25,26,27,28-tetrol, for example, calculations by AMBER 3.0 predict that the energy difference between cone

and other three conformers is greater than 7 kcal mol^{-1} whereas the results of MM2 predict that the difference is only 0.96 - 3.18 kcal mol^{-1}.[3] While, the ^1H NMR studies show that in most solvents only cone exists.[7] The discrepancy means that the exceptional stability of the cone form, which arises from intramolecular hydrogen-bonding interactions, is not adequately reproduced by MM2. Also misinterpreted is the relative stability of 25,26,27,28-tetramethoxycalix[4]arene and its *p-tert*-butyl derivative. Both AMBER 3.0 and MM2 predict that the relative stability of four conformers appears in the order of 1,3-alternate (most stable) > partial cone > cone > 1,2-alternate (least stable).[3] In contrast, the experimental findings reveal that cone and partial cone are more stable than 1,2-alternate and 1,3-alternate.[2,10,11]

We previously showed that the contradictory problems on 25,26,27,28-tetramethoxycalix[4]arene and its *p-tert*-butyl derivative can be solved to some extent by using a new algorism, MM3(89).[12] Furthermore, the effects of 5,11,17,23- and 25,26,27,28-substituents on the relative stability of four conformers of calix[4]arene were discussed using MM3(89).[13] It was shown that substituents in the lower rim site have a decisive role in ranking the relative stability of four conformers while those in the upper rim site only slightly affect the energy differences among conformers. These publications straightforwardly demonstrate the superiority of MM3(89) force field in which the π-aromatic system is taken into consideration over MM2 in which that is not taken into consideration.[12,13] As a next research object for our computational studies we decided to take up OH-depleted calix[4]arenes because of several reasons. Firstly, MM3(92), a well-refined version of MM3(89) is now available in which the contribution of hydrogen-bonding interactions is extensively taken into consideration.[14] Although computational studies of OH-depleted calix[4]arenes with MM2 or MMX have partly been reported by Biali *et al.*,[15] Fukazawa *et al.*[16] and others,[17] we considered it to be of great significance to re-examine the relative stability of calix[4]arenes and their OH-depleted calix[4]arenes by using MM3(92). Secondly, it is known that in calix[4]arene-25,26,27,28-tetrols a cone conformer is particularly stabilized by the intramolecular hydrogen-bonding interactions.[7-9,12,13] Our previous study has predicted that the bulkiness of the substituent in the lower rim site governs the relative stability of four conformers.[13] This means that to systematically discuss the relative stability one has to take both the steric effect which destabilizes the cone and the intramolecular hydrogen-bonding effect which stabilizes the cone into account. Thirdly, it is now possible to synthesize various OH-depleted calix[4]arenes by phosphorylation of OH groups followed by treatment with K/NH_3.[15-21] One can now enjoy the combination of NMR spectroscopy and MM3 studies. In this paper we report computational studies of 12 calix[4]arenes including *p*-H and *p-tert*-butyl series (**0a** ~ **4a** and **0b** ~ **4b** in scheme 1) and NMR spectroscopic studies on several compounds and discuss how precisely MM3(92) can reproduce the relative stability of four conformers.

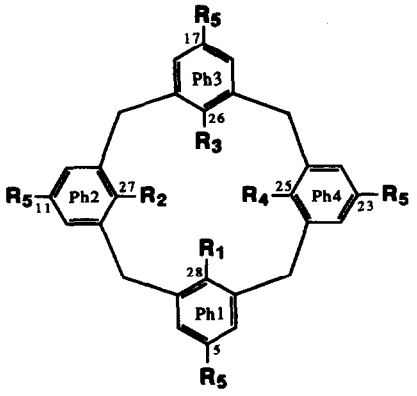

	R_1	R_2	R_3	R_4	R_5
0a	OH	OH	OH	OH	H
1a	H	OH	OH	OH	H
2a	H	OH	H	OH	H
2'a	H	H	OH	OH	H
3a	H	H	H	OH	H
4a	H	H	H	H	H
0b	OH	OH	OH	OH	Bu^t
1b	H	OH	OH	OH	Bu^t
2b	H	OH	H	OH	Bu^t
2'b	H	H	OH	OH	Bu^t
3b	H	H	H	OH	Bu^t
4b	H	H	H	H	Bu^t

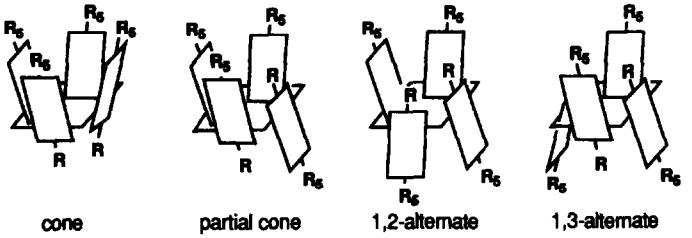

Scheme 1

Computational Technique

A new molecular mechanics calculation MM3(92)[14,22] was employed in this study. Input structures for calculations were generated by systematic modifications of MM3(89)-optimized structures of calix[4]arenes and [1$_4$]-methacyclophanes obtained in our previous work,[13] using a molecular modelling system (MOLGRAPH[23]). All aromatic carbons in the phenyl units of the calix[4]arene skeleton were treated as a conjugated π-system. The atom type number for hydrogen of the phenolic OH unit was set to 73: this atom type is newly added in MM3(92) force field[14] for an enol or a phenol hydrogen. Moreover, a special function and parameters for the hydrogen-bonding interaction are established in this version of MM3 force field.[14] Energy optimizations were carried out using a full matrix Newton-Raphson minimization method, followed by checking the eigenvalues of each Hessian matrix. These calculations were performed on a UNIX workstation system: SUN 4/2GX - IRIS 4D/35G. MOLGRAPH[23] was also used to analyze the geometry of optimized structures. The structures for each conformer reported in this paper are those of the lowest energy minima obtained by the grid search for the rotation of all substituents considering the molecular symmetries.

The NMR line-shape analysis program DNMR5[24] was used to establish the rate constant, effective transverse relaxation time and another parameters of mutual exchange effects on NMR bandshapes of OH-depleted calix[4]arenes. We applied this methodology to the mutual exchange process of bridging methylene protons (chemical exchange between axial and equatorial protons in

$ArCH_2Ar$, A $\rightleftharpoons$ B) of **2b** and **3b** in CD_2Cl_2 by the least-square fitting to their experimental spectra at various temperatures. These calculations were also carried out on the UNIX workstation system using the experimental data directly transferred from the NMR measuring system.

Materials

Procedures for the Synthesis of OH-depleted Calix[4]arenes (1b ~ 4b). OH-depleted calix[4]arenes **1b ~ 4b** were prepared by selective phosphorylation of *p-tert*-butylcalix[4]arene-25,26,27,28-tetrol **0b** followed by treatment with K/NH_3, using the similar manner described in the previous paper.[15-21] The synthesis of di-OH-depleted-*p-tert*-butylcalix[4]arene **2b** was described previously.[21] Here we describe the synthesis of tri-OH-depleted-*p-tert*-butylcalix[4]arene **3b.**

Preparation of p-tert-butylcalix[4]arene triphosphate. To a suspension of *p-tert*-butylcalix[4]arene-25,26,27,28-tetrol **0b** (3.0 g, 4.6 mmol) in diethyl ether (60 ml), 20 % NaOH aqueous solution (50 ml) was added. With vigorous stirring, a solution of diethyl chlorophosphate (2.0 g, 13.8 mmol) in diethyl ether (15 ml) was added dropwise over a period of 2 h at room temperature. The ether layer was separated and washed with water several times. After drying over Na_2SO_4, the filtrate was concentrated to dryness and the product was isolated using silica gel column chromatography (eluent; $CHCl_3$:MeOH = 1:0 to 9:1 v/v). *p-tert*-Butylcalix[4]arene triphosphate (3.4 g) was isolated in 69.5 % yield.

Preparation of tri-OH-depleted-p-tert-butylcalix[4]arene 3b. A reaction vessel equipped with a cold-finger condenser was charged with 50 ml of NH_3 at -78 °C. Potassium metal (3.0g, 75 mmol) was added carefully to this solution. An ether solution (10 ml) of *p-tert*-butylcalix[4]arene triphosphate (1.4 g, 1.3 mmol) was added dropwise to the blue NH_3 solution at -78°C. After 20 min, NH_4Cl (6.0 g) was added carefully until the blue color was discharged. NH_3 was evaporated off and the residue was extracted with ether. After purification by column chromatography (silica gel, eluent; hexane:$CHCl_3$ = 4:1 to 1:1 v/v), tri-OH-depleted-*p-tert*-butylcalix[4]arene **3b** (0.22 g) was afforded in 28 % yield as white powder, mp 226 - 229 °C; IR (KBr) ν_{OH} 3510 cm^{-1}; ^1H NMR(CD_2Cl_2, 25°C), δ 1.26, 1.29 and 1.31 (Bu^t, s each, 9H, 9H and 18H, respectively), 3.76 and 3.90 ($ArCH_2Ar$, s each, 4H each), 4.41 (OH, broad, 1H), 6.44, 6.51 (ArH, s each, 1H and 2H, respectively), 7.05, 7.09, 7.13 and 7.20 (ArH, d, s, d and d, respectively, 2H each) as shown in Figs. 2 and 3 ; ^{13}C NMR, δ 31.5 and 31.7 ($-CH_3$), 34.2, 34.7 and 34.8 (>C<), 38.0 and 43.0 (Ar-C-Ar), 123.7, 123.9, 124.4, 125.0, 125.7, 126.7, 127.2, 140.8, 141.7, 142.3, 143.5, 150.3, 151.7, and 151.9 (ArC); Anal. calculated for $C_{44}H_{56}O$: C, 87.94, H, 9.39. Found: C, 86.86, H, 9.41.

Miscellaneous. The ^1H NMR apparatus used here was a Bruker ARX300 spectrophotometer. The IR spectrum is measured by Shimazu FTIR-8100M infrared spectrophotometer.

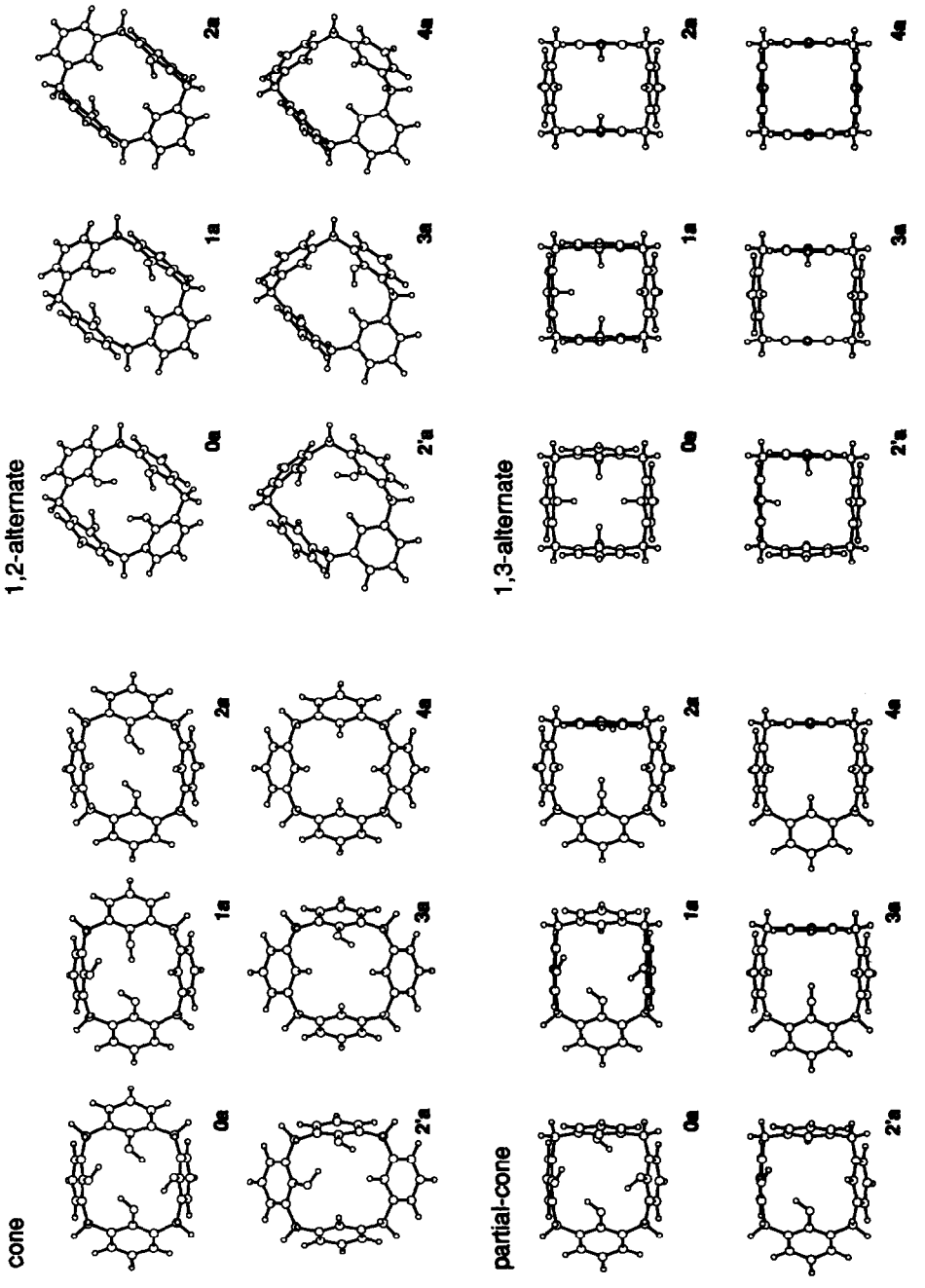

Fig. 1 MM3(92) optimized structures for four conformers in **0a** - **4a**

Results and Discussion

Results of MM3 Calculations. The MM3-calculated relative potential energies and molecular symmetries of the four main conformational isomers of OH-depleted calix[4]arenes are given in Table 1. In some cases the difference in the steric energy is as small as 0.1 kcal mol^{-1}, which is not so significant in the experimental stability of calix[4]arenes. However, each energy term such as bending term, van der Waals term, torsional term, etc. is very different, so that we include these values in Table 1. There are several ways in which the conformation of a calix[4]arene molecule can be described. In Tables 2-1 through 2-4 we summarize the conformational features of **0a** ~ **4a** obtained with MM3 optimization, including the inclination of the phenyl rings with respect to the best plane of the four methylene groups chosen as a reference plane,[25] bond angles between neighboring phenyl rings centered on the methylene carbon atoms, and the distances between the distal methylene carbon atoms. Drawings of the MM3 optimized structures of these compounds are also shown in Fig. 1.

Table 1. MM3-calculated steric energies (relative energy) (E)[a] and symmetry (PG)[b] of the four main conformers of OH-depleted calix[4]arenes

Calix[4]arene	Cone		Partial Cone		1,2-Alternate		1,3-Alternate	
	E	PG	E	PG	E	PG	E	PG
0 a	10.2 (0.0)	C_2[c]	15.8 (5.6)	C_1	16.3 (6.1)	C_i	20.8(10.6)	D_{2d}
1 a	13.7 (0.0)	C_1	16.2 (2.5)	C_1	18.3 (4.6)	C_1	21.0 (7.3)	C_s
2 a	18.0 (0.0)	C_2	18.3 (0.3)	C_1	19.9 (1.9)	C_i	20.1 (2.1)	C_{2v}
2'a	17.8 (0.0)	C_1	18.2 (0.4)	C_1	18.2 (0.4)	C_1	21.5 (3.7)	C_2
3 a	20.2 (0.3)	C_1	19.9 (0.0)	C_s	21.0 (1.1)	C_1	21.1 (1.2)	C_s
4 a	20.0 (0.0)	C_{4v}	21.2 (1.2)	C_s	21.8 (1.8)	C_1	21.7 (1.7)	D_{2d}
0 b	19.1 (0.0)	C_2	25.2 (6.1)	C_1	26.6 (7.5)	C_1	31.9(12.8)	C_1
1 b	24.1 (0.0)	C_1	26.0 (1.9)	C_1	28.8 (4.7)	C_1	31.1 (7.0)	C_1
2 b	28.7 (0.5)	C_1	28.2 (0.0)	C_1	30.6 (2.4)	C_1	30.9 (2.7)	C_2
2'b	27.9 (0.0)	C_1	28.0 (0.1)	C_1	29.0 (1.1)	C_1	30.5 (2.6)	C_1
3 b	30.4 (0.6)	C_1	29.8 (0.0)	C_1	32.0 (2.2)	C_1	31.3 (1.5)	C_1
4 b	30.6 (0.0)	C_4	31.6 (1.0)	C_1	33.1 (2.5)	C_1	31.7 (1.1)	S_4

[a] Energies in kcal mol^{-1}. The values in parentheses are the energy differences from the most stable conformation. [b] Symmetry point group for the optimized structures. When taking only a [14]methacyclophane skeleton without OH and Bu^t into account, the symmetry expressed with C_2 or C_4 becomes C_{2v} or C_{4v}. The direction of OH or Bu^t reduces the symmetry to C_2 or C_4. [c] The steric energy for the C_4 structure of cone-**0a** is 10.8 kcal mol^{-1}.

Table 2-1. Geometries of MM3 optimized 'cone-type' structures

	0a	**1a**	**2a**	**2'a**	**3a**	**4a**
Plane Angle[d] /deg						
Ph_1	* 77.1	69.2	73.0	41.8	47.1	53.6
Ph_2	* 48.4	* 47.2	* 45.0	65.5	61.1	53.6
Ph_3	* 77.1	* 76.8	73.0	* 50.7	46.5	53.6
Ph_4	* 48.4	* 44.3	* 45.0	* 73.6	* 66.7	53.6
Angle /deg						
Ph_1-CH_2-Ph_2	112.4	112.9	112.2	113.9	113.1	113.2
Ph_2-CH_2-Ph_3	112.9	112.7	113.7	112.7	113.5	113.2
Ph_3-CH_2-Ph_4	112.4	112.2	112.2	112.5	112.6	113.2
Ph_4-CH_2-Ph_1	112.9	113.0	113.7	112.7	113.0	113.2
Distance[e] /Å						
C(1,2)-C(3,4)	7.31	7.29	7.42	7.05	7.25	7.15
C(2,3)-C(4,1)	7.17	7.13	6.94	7.34	7.10	7.15

Table 2-2. Geometries of MM3 optimized 'partial cone-type' structures

	0a	1a	2a	2'a	3a	4a
Plane Angle[d] /deg						
Ph_1	* 74.6	-72.8	71.6	-78.4	77.2	77.5
Ph_2	* 48.9	* 84.0	* 43.2	73.0	-102.8	33.5
Ph_3	* 83.8	* 44.4	74.0	* 44.8	77.2	77.5
Ph_4	* -79.6	* 88.1	* -94.8	* 91.0	* 41.4	-88.3
Angle /deg						
Ph_1-CH_2-Ph_2	112.1	115.7	112.3	116.2	113.3	112.8
Ph_2-CH_2-Ph_3	112.2	111.5	112.3	111.6	113.3	112.8
Ph_3-CH_2-Ph_4	116.4	111.8	113.5	112.3	111.9	113.6
Ph_4-CH_2-Ph_1	117.6	115.7	114.2	114.6	111.9	113.6
Distance[e] /Å						
C(1,2)-C(3,4)	7.22	7.22	7.19	7.18	7.15	7.14
C(2,3)-C(4,1)	7.26	7.20	7.15	7.18	7.15	7.14

Table 2-3. Geometries of MM3 optimized '1,2-alternate-type' structures

	0a	1a	2a	2'a	3a	4a
Plane Angle[d] /deg						
Ph_1	* -51.4	-37.1	-38.5	-11.3	-28.4	17.3
Ph_2	* -75.1	* -76.5	* -82.0	-75.4	-83.5	-81.9
Ph_3	* 51.4	* 55.6	38.5	* 82.2	51.0	72.9
Ph_4	* 75.1	* 80.0	* 82.0	* 68.7	* 76.0	61.6
Plane Angle[f] /deg						
Ph_1	-51.4	-40.9	-38.5	-16.9	-22.7	1.1
Ph_2	-75.1	-80.5	-82.0	-87.7	-88.0	-93.7
Ph_3	51.4	51.5	38.5	70.2	58.0	60.4
Ph_4	75.1	76.0	82.0	56.3	57.4	48.8
Angle /deg						
Ph_1-CH_2-Ph_2	112.8	112.6	112.5	114.7	112.5	114.6
Ph_2-CH_2-Ph_3	119.8	119.1	117.6	113.7	116.2	114.4
Ph_3-CH_2-Ph_4	112.8	112.1	112.5	112.5	112.8	112.7
Ph_4-CH_2-Ph_1	119.8	117.6	117.6	115.5	117.5	113.8
Distance[e] /Å						
C(1,2)-C(3,4)	6.89	6.85	6.85	6.74	6.76	6.91
C(2,3)-C(4,1)	7.61	7.57	7.54	7.35	7.54	7.05

Table 2-4. Geometries of MM3 optimized '1,3-alternate-type' structures

	0a	1a	2a	2'a	3a	4a
Plane Angle[d] /deg						
Ph_1	* 80.0	76.5	78.2	80.7	80.8	87.8
Ph_2	* -80.0	* -84.2	* -91.2	-80.7	-90.6	-87.8
Ph_3	* 80.0	* 83.5	78.2	* 87.0	80.8	87.8
Ph_4	* -80.0	* -84.2	* -91.2	* -87.0	* -92.0	-87.8
Angle /deg						
Ph_1-CH_2-Ph_2	115.3	114.9	113.3	114.8	113.2	112.6
Ph_2-CH_2-Ph_3	115.3	114.1	113.3	113.9	113.2	112.6
Ph_3-CH_2-Ph_4	115.3	114.1	113.3	113.2	112.9	112.6
Ph_4-CH_2-Ph_1	115.3	114.9	113.3	113.9	112.9	112.6
Distance[e] /Å						
C(1,2)-C(3,4)	7.22	7.19	7.15	7.17	7.14	7.12
C(2,3)-C(4,1)	7.22	7.19	7.15	7.17	7.14	7.12

[d] Dihedral angle between the phenyl plane and the mean plane of four methylene carbons.

[e] Distance between two distal methylene carbons: C(*x*,*y*) indicates the methylene carbon connecting Phx and Phy. [f] Dihedral angle between the phenyl plane and the 'new reference plane'.[25]

* denotes the phenyl ring with an OH substituent (phenol unit).

We can raise a number of intriguing points about the data recorded in Table 1. Firstly, in **0a** and **0b** the order of the relative stability estimated from the steric energy is in the order of cone > partial cone > 1,2-alternate > 1,3-alternate and the difference between cone and partial cone is particularly large (5.6 kcal mol^{-1} for **0a** and 6.1 kcal mol^{-1} for **0b**). This is, of course, due to the difference in the number of possible hydrogen-bonds, four for cone and two for partial cone. These energy gaps are large enough to explain the experimental fact that only the cone species is detectable by NMR spectroscopy in solution.[7-9] Very interestingly, MM3(92) reports that the most stable structure of cone-**0a** and cone-**0b** is not C_4 symmetry but C_2 symmetry.[26] The structure with C4 symmetry includes one imaginary frequency (or one negative eigenvalue of the Hessian matrix) among 3N-6. This means that this structure corresponds to a transition state on MM3(92) potential surface. In cone-**0a**, for example, the C_2 structure is more stable by 0.6 kcal mol^{-1} than the C_4 structure. It is known that in tetramethoxycalix[4]arene without the intramolecular hydrogen-bonding interaction among OH groups the cone conformation with C_2 symmetry is the most stable.[3,12] The superiority of C_2 over C_4 is explained as such that in the cone conformation C_2 can reduce the steric crowding in the lower rim more efficiently than C_4.[12] Obviously, the OH groups in cone-**0a** and cone-**0b** not only stabilize the cone conformation by the intramolecular hydrogen-bonds but also increase the steric crowding in the lower rim.

Secondly, with depleting OH groups the energy difference between cone and other three conformations becomes smaller: in mono-OH-depleted **1a** and **1b** the cone conformation is still most stable but in di-OH-depleted **2a** (or **2'a**) and **2b** (or **2'b**) the stability of cone is almost comparable with that of partial cone. Hence, if two OH-carrying phenyl units adopt a *syn* conformation there is no essential difference in the hydrogen-bonding stabilization effect between cone and partial cone.

Thirdly, in tetra-OH-depleted calix[4]arene (**4a** and **4b**) the most stable conformation is cone with C_4 symmetry whereas in calix[4]arene-25,26,27,28-tetrols (**0a** and **0b**) the most stable conformation is cone with C_2 symmetry consisting of two standing-up phenyl units and two flattened phenyl units. This means that the calix[4]arene framework with no substituent in the lower rim favors a C_4 symmetrical ring and C_2 symmetry adopted by **0a** and **0b** is due to the formation of stable hydrogen-bonds and/or to relaxing the steric crowding among OH groups.[12] It is reported that in solution the NMR spectra of calix[4]arene-25,26,27,28-tetrols appear as a C_4 symmetrical structure but there is no experimental evidence so far if they adopt the regular C_4 symmetrical structure or enjoy C_2-C_2 interconversion faster than the NMR time-scale.[26] Also, it is worthwhile to mention that in a cone conformation of di-OH-depleted calix[4]arenes distally-depleted **2a** and **2b** are less stable by 0.2 and 0.8 kcal mol^{-1} than proximally-depleted **2'a** and **2'b**. Examination of Table 2-1 and Fig. 1 reveals that cone-**2a** adopts C_2 symmetry like cone-**0a** but the two distal phenyl units are more flattened. As shown in Fig. 1 and δ_{OH} in ^1H NMR spectroscopy (4.2 ppm in CD_2Cl_2 : see below), these two OH groups do not form an intramolecular hydrogen-bond. So, the flattening should be caused to reduce the steric crowding between OH groups and hydrogen atoms in the $ArCH_2Ar$ groups. On the other hand, cone-**2'a** forms an intramolecular hydrogen-bond between the two proximal phenol units. Although it only has C_1 symmetry and includes a extremely flattened Ph_1, it is more stable than cone-**2a** with flattened C_2 symmetry.

Fourthly, examination of each energy term (data not shown here but deposited as supplementary material) shows that in the torsional term cone-**4a** is more stable by 2.1 kcal mol^{-1} than partial-cone-**4a** whereas in the dipole-dipole interaction term partial-cone-**4a** is more stable by 1.3 kcal mol^{-1} than cone-**4a**. This means that the dihedral angle between benzene rings in the cone skeleton is more favorable than that in the partial cone skeleton but the cone skeleton with four dipoles oriented into the same direction is less favorable than the partial cone skeleton with one dipole inverted against other three dipoles. In totally including other terms, cone-**4a** is more stable by 1.2 kcal mol^{-1} than partial-cone-**4a**. In **3a**, on the other hand, partial-cone-**3a** is more stable than cone-**3a** (by 0.3 kcal mol^{-1}). They show the similar trend for the torsional and dipole-dipole interaction terms as **4a** but in the van der Waals term cone-**3a** is less stable by 2.9 kcal mol^{-1} than partial-cone-**3a** and this difference causes a reversal in the relative stability between cone and partial cone. The van der Waals destabilization of cone-**3a** arises from steric repulsion between the oxygen atom in 25-OH and the two axial hydrogen atoms in CH_2ArCH_2 (their interatomic distances in the MM3-optimized structure are 2.45 and 2.63 Å) and between the hydrogen atom in 25-OH and the 28-H in ArH (2.12 Å) or a neighboring axial hydrogen atom (2.08 Å). These results indicate that the substitution of ArH at 25,26,27,28-positions with OH certainly increases the steric crowding in the cone conformation. Thus, the cone can become the most stable conformation when the hydrogen-bonding stabilization effect overcomes the van der Waals destabilization effect.

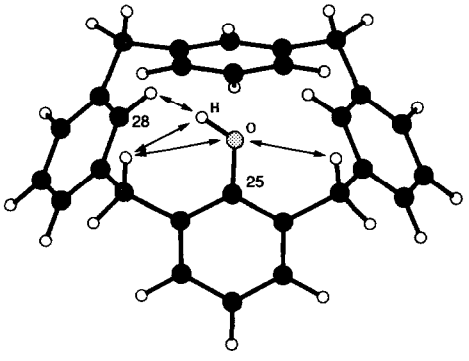

Fifthly, it is interesting to assess which phenyl unit (ArOH or ArH) rotates in the partial cone conformation and which phenyl units take the same side of the ring in the 1,2-alternate conformation. As shown in Table 2-2 and Fig. 1, partial-cone-**1a** has an OH-depleted phenyl unit inverted to other three phenol units. This conformation is most energetically-favorable to hold the high hydrogen-bonding probability, OH··OH··OH. In partial-cone-**2'a** an OH-depleted phenyl unit is inverted so that it can enjoy hydrogen-bonding interaction, OH··OH between the proximal phenol units in the same side of the ring. In partial-cone-**2a**, on the other hand, an OH-carrying phenol unit is inverted. Probably, two distal phenol units cannot be flattened to form an intramolecular hydrogen-bond even though they are held in the same side of the ring by rotating an OH-depleted phenyl unit. The similar inversion selectivity is seen for the 1,2-alternate conformation. In 1,2-alternate-**2'a** two proximal phenol units reside in the same side of the ring to form an intramolecular hydrogen-bond whereas in 1,2-alternate-**2a** two distal phenol units reside in the opposite side of the ring due to the difficulty to form an intramolecular hydrogen-bond.

Lastly, introduction of *tert*-butyl groups into the *para*-positions changes the relative stability only to a smaller extent. The difference in the relative stability between **a** and **b** series is seen only for **2** and **3** : in **2a** cone > partial cone > 1,2-alternate > 1,3-alternate whereas in **2b** partial cone >

cone > 1,2-alternate > 1,3-alternate and in **3a** partial cone > cone > 1,2-alternate > 1,3-alternate whereas in **3b** partial cone > cone > 1,3-alternate > 1,2-alternate. Even in these series the differences in the steric energies are relatively small.

In Table 1 and Fig. 1 we also referred to the molecular symmetry of each conformer. Cone conformers tend to adopt C_{2v} symmetry except **4a** with C_{4v} symmetry. Partial cone and 1,3-alternate conformers tend to adopt C_s and D_{2d} or their resemblance modified by the slight change in the OH groups, respectively. The 1,2-alternate conformers deserve special attention due to their unique molecular symmetries. Compounds **0a**, **1a** and **2a** (**0b**, **1b** and **2b**) adopt regular Ci symmetry whereas **2'a**, **3a** and **4a** (also **2'b**, **3b** and **4b**) adopt unique C_1 symmetry in which four bridge methylene carbons do not exist in the same plane. Probably, C_1 symmetrical 1,2-alternate calix[4]arenes for these compounds are subject to C_1-C_1 interconversion via C_i : that is, C_i corresponds to a transition state for C_1-C_1 interconversion. In fact, the structure with C_i symmetry includes one imaginary vibrational frequency. Thermodynamic parameters for each structure were obtained from MM3(92) computation using a full-matrix Newton-Raphson minimization method (deposited in Supplementary Material). In 1,2-alternate-**4a**, for example, C_1 is more stabilized by 1.6 kcal mol^{-1} in the steric energy and by 3.2 kcal mol^{-1} in the free energy at 298.16 K than C_i. Comparison of the energy terms (the data are also deposited in Supplementary Material) discloses that C_1 is less advantageous by 0.5 kcal mol^{-1} in the dipole-dipole interaction term but more advantageous by 1.0 kcal mol^{-1} in the torsional term and by 0.4 kcal mol^{-1} in the bending term. This implies that the C_1 framework consists of more favorable dihedral angles.

In Fig. 1 it is worthy to pay special attention to the direction of OH groups. When a hydrogen bond can be formed between two proximal OH groups, the OH group is exactly directed toward the oxygen atom in the neighboring OH group. In 1,3-alternate conformers, on the other hand, there exist no such two proximal OH groups with a *syn* conformation. Previously, we computed the energy-optimized structure for 1,3-alternate-**0a** with MM3(89).[13] Therein, the OH groups are all directed toward the proximal inverted phenyl rings, the angle between the OH and the benzene plane being 38.8°.[13] The symmetry is S_4. In the present system computed with MM3(92) force field, the OH groups are all directed to the center of the calix[4]arene ring, the angle between the OH and the benzene plane being close to 90°. The symmetry is D_{2d}.

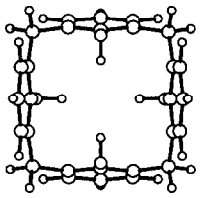

D_{2d}

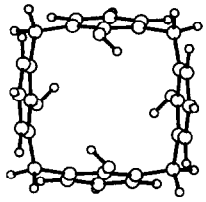

S_4

To explain this discrepancy we carefully checked the energy terms for these two structures. As for the steric energy D_{2d} (20.8 kcal mol^{-1}) is more stable by 0.6 kcal mol^{-1} than S_4 (21.4 kcal mol^{-1}). In each energy term, the compression term and the bending term for D_{2d} are stabilized by 0.6 and 2.1 kcal mol^{-1}, respectively. This is due to the reduction of the torsion in the metacyclophane skeleton on going from S_4 to D_{2d}. The van der Waals term (by 4.2 kcal mol^{-1})

and the dipole-dipole interaction term (by 1.6 kcal mol^{-1}) are also stabilized. The stabilization effect in the van der Waals term is mostly related to the hydrogen-bonding term which is newly introduced in MM3(92). When the direction of the OH group is parallel to the proximal benzene rings (D_{2d} structure), it can earn the largest stabilization from the dipole-dipole interaction term. These specifications well explain the superiority of D_{2d} over S_4 for 1,3-alternate-**0a**.

Results of NMR Spectroscopic Studies. Biali *et al.*[15] succeeded in X-ray analysis of **1b**, **2b** and **4b**. Crystal **1b** was obtained as a cone conformer, which is in accord with the most stable conformer predicted by the present MM3 computation. On the other hand, crystal **2b** and **4b** were obtained as a 1,2-alternate conformer, which is not the most stable conformer (see Table 1). Particularly, 1,2-alternate-**2b** is the least stable among four possible conformers. Furthermore, 1,2-alternate-**4b** in the crystal adopts conventional C_i symmetry but not C_1 symmetry predicted to be more stable by MM3 computation. These discrepancies are probably due to the crystal packing force, a special energy term operating only in the crystal phase. Since the theoretical calculation usually assumes an isolated molecule in the ideal gas phase, the structures determined in solution should be more or less suitable to comparison with the computational data. We thus estimated the structures of **0b**, **1b**, **2b**, **3b** and **4b** in solution by ^1H NMR spectroscopy.

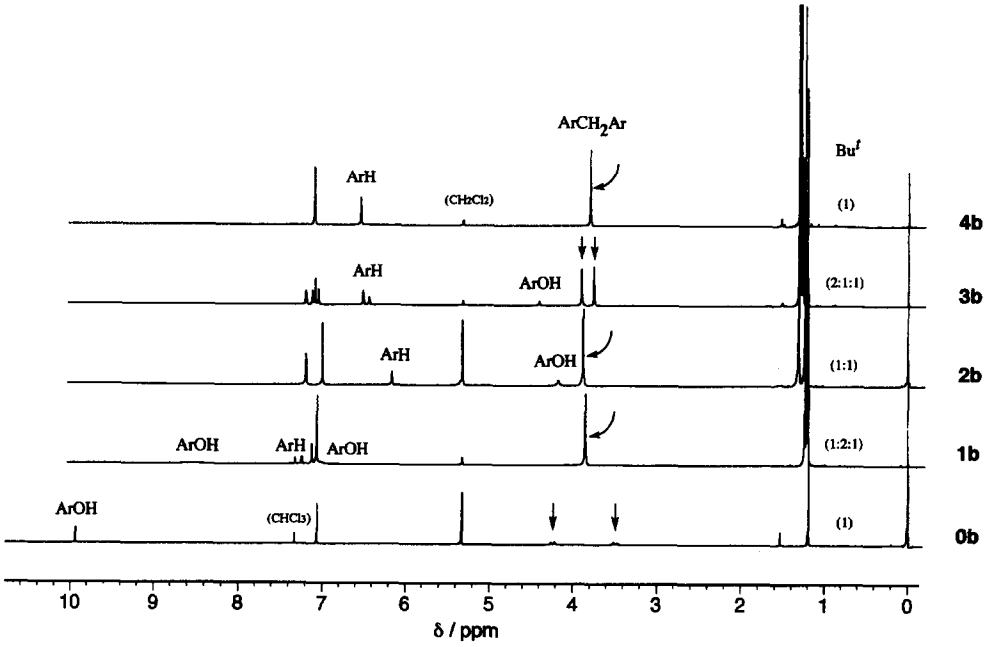

Fig. 2. ^1H NMR spectra of **0b** - **4b** in CD_2Cl_2 at room temperature.
Arrows indicate proton signals assignable to $ArCH_2Ar$ methylene protons.

In Fig. 2 ^{1}H NMR spectra (300 MHz, CD_2Cl_2) of five compounds measured at room temperature are illustrated. The $ArCH_2Ar$ proton signals, which are most convenient to assign the calix[4]arene conformation, appear at 3.4 - 4.8 ppm. In **0b** they appear as a pair of doublets at 3.49 and 4.23 ppm characteristic of a cone conformation. Compounds **2b** and **4b** afford a singlet resonance at 3.88 and 3.80 ppm, respectively. The results imply that in **2b** and **4b** the exchange rates among possible conformers are faster than the NMR time-scale at room temperature. Compounds **1b** has two inequivalent $ArCH_2Ar$ methylene groups, so that even though the exchange rates are faster than the NMR time-scale, they should appear as two singlet peaks. As shown in Fig. 2, however, they apparently afford one singlet peak at 3.85 ppm. This is due to an accidental coincidence of the two chemical shifts. In fact, we could observe two separate singlet peaks at 3.86 and 3.90 ppm in $CDCl_3$. Compound **3b** also has two inequivalent $ArCH_2Ar$ methylene groups. In this case, they appear as two singlet peaks with a 1:1 integral intensity ratio.

The chemical shifts of the OH protons (δ_{OH}) are also interesting. It is known that in general, the OH forming a strong hydrogen bond appears at lower magnetic field. As seen in Fig. 2, δ_{OH} values are 9.9 ppm (4H) for **0b**, 7.1 ppm (2H) and 8.6 ppm (1H) for **1b**, 4.2 ppm (2H) for **2b** and 4.4 ppm (1H) for **3b** in CD_2Cl_2 at room temperature. The data show that **0b** possesses an exceptionally strong, circular hydrogen-bonds. In **1b**, the central OH proton for HO··HO··HO $\rightleftharpoons$ OH··OH··OH is included in the hydrogen-bond stronger than other two terminal OH protons. On the other hand, **2b** and **3b** which scarcely form or cannot form a hydrogen-bond give the δ_{OH} at relatively high magnetic field. The similar trend was observable for IR spectra of each conformer. In CCl_4 at 16 mmol dm^{-3} the ν_{OH} peaks appear at 3340 and 3450 cm^{-1} for **1b**, 3530 cm^{-1} for **2b** and 3540 cm^{-1} for **3b**. The ν_{OH} values for **1b** was concentration-dependent, indicating the presence of the intermolecular hydrogen-bonding interaction.

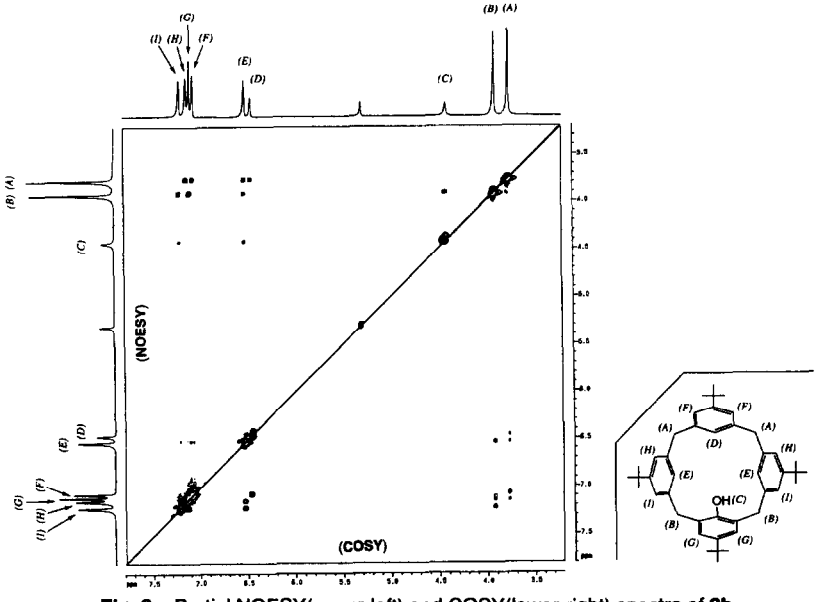

Fig. 3. Partial NOESY(upper-left) and COSY(lower-right) spectra of **3b** (300 MHz, CD_2Cl_2, r. t.)

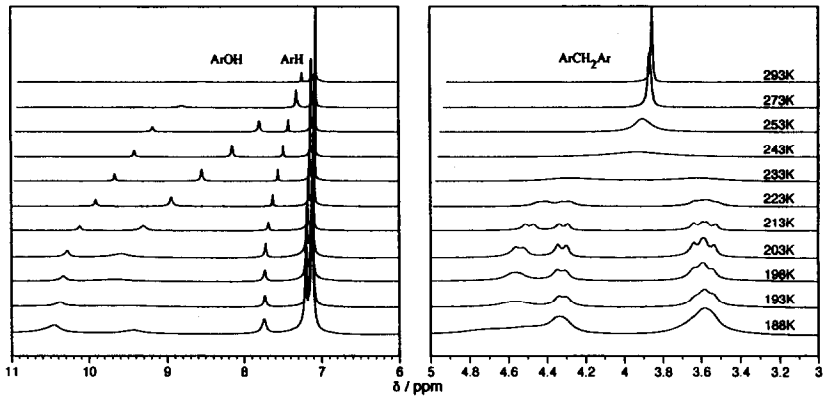

Fig. 4-1 Temperature dependence of the ^1H NMR spectra for **1b** (300 MHz, CD_2Cl_2)

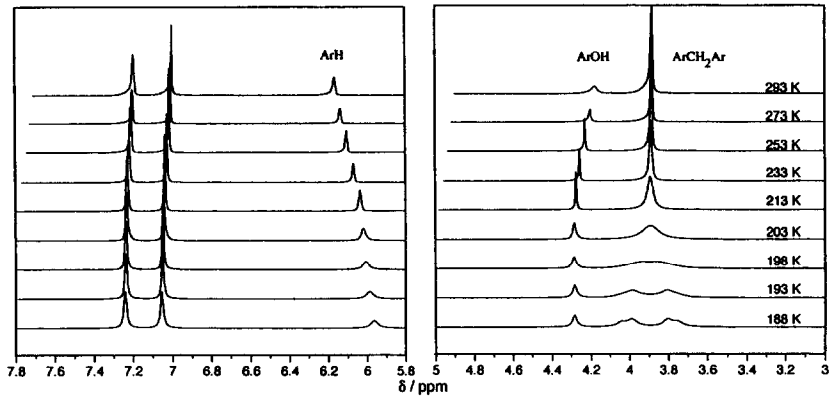

Fig. 4-2 Temperature dependence of the ^1H NMR spectra for **2b** (300 MHz, CD_2Cl_2)

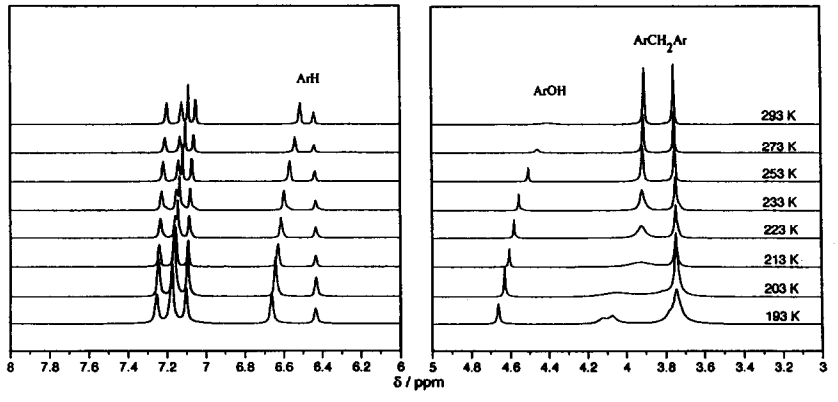

Fig. 4-3 Temperature dependence of the ^1H NMR spectra for **3b** (300 MHz, CD_2Cl_2)

Figure 3 shows NOESY and COSY spectra (300 MHz, CD_2Cl_2) of **3b** at room temperature. The significant cross peaks are detected for between methylene protons (A) and aromatic protons (D, E, F and H) and between methylene protons (B) and aromatic protons (E, I and G). The OH proton (C) give the three cross peaks with aromatic protons (A, E and I) in a NOESY spectrum. One can expect significant steric repulsion among these protons, which is the origin of the van der Waals repulsion destabilizing cone-**3b** as found in the molecualr mechanics studies.

To further specify the stable conformation adopted by **1b** ~ **4b**, we measured the ^1H NMR spectra at lower temperature region. As shown in Figs. 4-1 ~ 4-3, the ^1H NMR spectra of **1b, 2b** and **3b** showed the clear temperature dependence. On the other hand, those of **4b** was scarcely affected by a temperature change: even at 188K the spectral pattern was virtually same as that at 293 K including sharp singlet peaks. It thus seems difficult to specify the conformer adopted by **4b** although the computational study (Table 1) predicts that the cone is the most stable among four possible conformations. In **1b** (Fig. 4-1) the singlet $ArCH_2Ar$ peak at room temperature is gradually broadened with lowering the medium temperature and eventually separated into two pairs of doublets at 213 K. Judging from the molecular symmetry, this splitting pattern is indicative of a cone conformation. The coalescence temperature (*Tc* : 300 MHz, CD_2Cl_2) is 240 K (compare with *Tc* = 246 K : 200 MHz, $CDCl_3$:CD_2Cl_2 = 1:1 v/v[17]). The result shows good agreement with the computational prediction (Table 1) that in **1b** the cone is more stable by more than 1.9 kcal mol^{-1} than other three conformations. The peak broadening observed at 188 K (Fig. 4-1) is probably due to the increased viscosity of CD_2Cl_2. In **2b** (Fig. 4-2) the $ArCH_2Ar$ signal changes from a singlet resonance to a pair of doublets via *Tc* = 200 K. Judging from the molecular symmetry **2b** should adopt either cone or 1,3-alternate. The ROESY spectrum at 188K could not be assigned by the structure of a single conformer but could be assigned reasonably by assuming a mixture of cone and 1,3-alternate. In **3b** the methylene peak at lower magnetic field split but that at higher magnetic field remained singlet even at 193 K. The ROESY spectrum at 193 K showed that this compound is also a mixture of two types of interconversion processes: interconversion between cone and partial cone and that between 1,3-alternate and partial cone. The *Tc* values obtained in these ^1H NMR measurements (300 MHz, CD_2Cl_2) are above 300 K for **0b**, 240 K for **1b**, 200 K for **2b**, 210 K for the lower magnetic field peak and below 193 K for the higher magnetic field peak in **3b** and below 188 K for **4b**: clearly, the *Tc* decreases with decreasing OH groups. This means that the OH group interferes with the rotation of phenyl units.

Here, we determined the thermodynamic parameters by simulating the temperature-dependent ^1H NMR spectra.* The simulation spectra are illustrated in Fig. 5. From the exchange rate constants (k) thus obtained, we calculated $\Delta H^{\neq}$, $\Delta S^{\neq}$ and $\Delta G^{\neq}$ according to the following equations. The results are summarized in Table 3. Araki *et al.*[27] reported the $\Delta G^{\neq}$ for **0a** and **0b** (at 298 K, $CDCl_3$) to be 15.7 and 16.4 kcal mol^{-1}, respectively. Hence, the $\Delta G^{\neq}$ values for **2b** and **3b** are smaller by 7.5 and 6.3 kcal mol^{-1}. Biali *et al.*[18] reported the $\Delta G^{\neq}$ (at 202 K, $CDCl_2F$) to be 9.6 kcal mol^{-1} for **2b**. This value is in good agreement with the present study.

$$\ln\frac{k}{T} = -\frac{\Delta H^{*}}{RT} + \frac{\Delta S^{*}}{R} - \ln\frac{h}{k_B}$$ (h: Planck const., k_B: Boltzmann const.)

* Fukazawa *et al.* have already analyzed the conformational properties of mono-OH-depleted calix[4]arene in detail,[16] so that we here omitted the simulation study of **1b**.

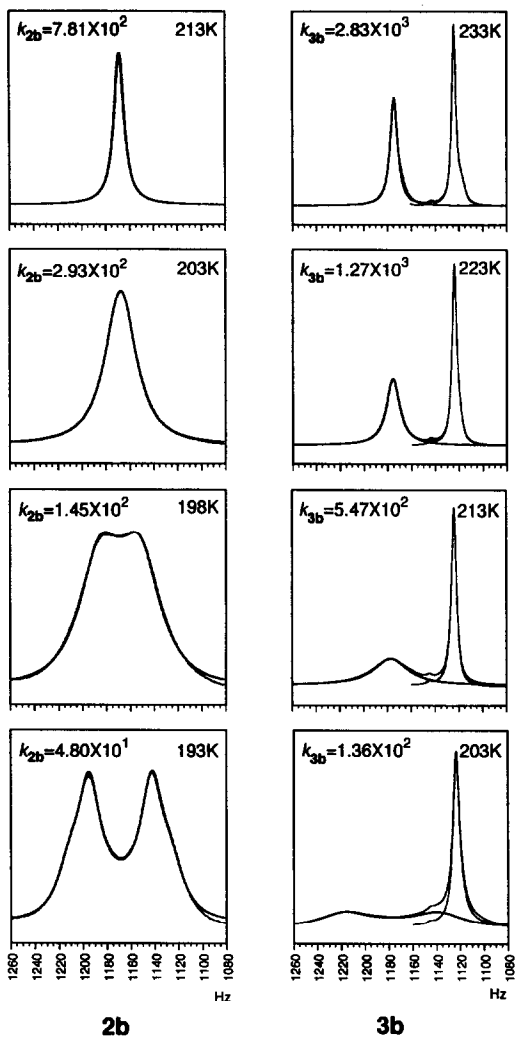

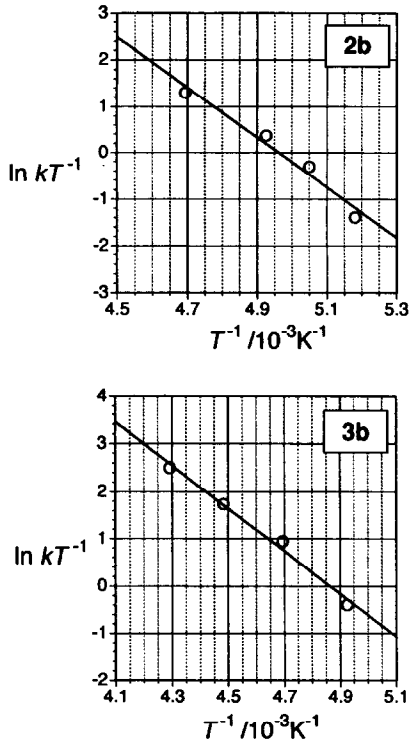

Fig. 6. Plot of ln kT^{-1} v.s. T^{-1} for the simulated value of exchange rate constants for **2b** and **3b**. (r=-0.984 and -0.994, respectively)

Fig. 5. Observed (300MHz, CD_2Cl_2: normal line) and simulated (bold line) ^{1}H-NMR spectra of $ArCH_2Ar$ proton for **2b** and **3b** at various temperatures (*k*: computed exchange rate constant).

Table 3. Thermodynamic parameters for the ring inversion of OH-depleted calixarenes

Calixarenes	Solvent	*Tc*	$\Delta H^{\neq}$ / kcal mol^{-1}	$\Delta S^{\neq}$ / cal mol^{-1} K^{-1}	$\Delta G^{\neq}_{Tc}$ / kcal mol^{-1}	$\Delta G^{\neq}_{298K}$ / kcal mol^{-1}
0b [a, 27]	$CDCl_3$	> 328 K	15.9	-1.7	-	16.4
2b [b]	CD_2Cl_2	200 K	10.7	5.91	9.5	8.9
3b [c]	CD_2Cl_2	210 K	8.96	-3.70	9.7	10.1

a Parameters for the cone $\rightleftharpoons$ cone interconversion process
b Parameters for the rotation of phenyl groups in cone and 1,3-alternate
c Parameters for the rotation of a phenol group

Concentration Dependence. Fukazawa *et al.*[14] already found that a mono-OH-depleted calix[4]arene forms a dimer through an intermolecular hydrogen-bond. In the ^{1}H NMR spectrum of **1b** at room temperature (Fig. 2), the δ_{OH} for the two terminal OH protons in HO··HO··HO $\rightleftharpoons$ OH··OH··OH appeared at very low magnetic field (7.1 ppm). It is reasonable to consider that this not only due to the intramolecular hydrogen-bonding interaction but due to the intermolecular one. We thus measured the ^{1}H NMR spectra of **1b**, **2b** and **3b** at 0.56 - 4.42 mmol dm^{-3}. As a result, it become clear that the spectra for **2b** and **3b** are scarcely affected by the concentration change whereas that for **1b** is concentration-dependent.

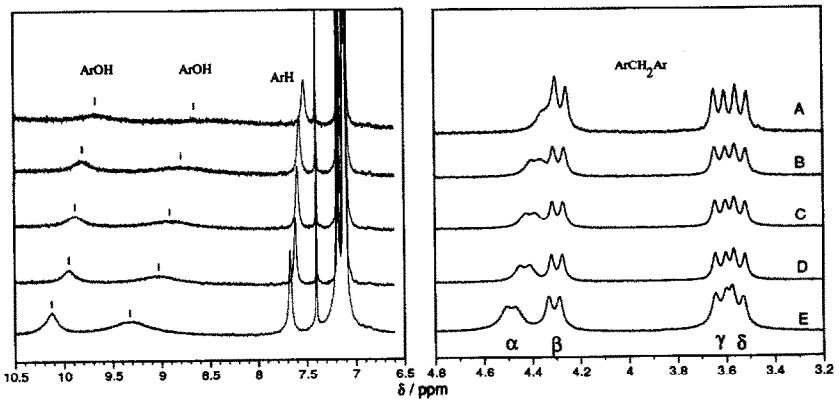

Fig. 7. Concentration dependence of the ^{1}H NMR spectra for **1b** in CD_2Cl_2 at 213K (A: 0.56, B: 1.11, C: 1.47, D: 2.21, E: 4.42 mmol dm^{-3})

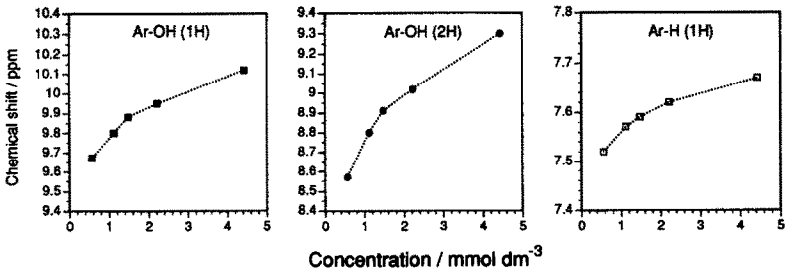

Fig. 8. Concentration dependence of δ_{ArOH} and δ_{ArH} of **1b** (CD_2Cl_2, 213K)

Figure 7 shows the ^{1}H NMR spectrum for **1b** in various concentrations at 213 K. In Fig. 8 δ_{OH} and δ_{ArH} are plotted against **1b** concentration. It is seen from these figures that with increasing **1b** concentration the chemical shifts move to lower magnetic field. For the $ArCH_2Ar$ methylene protons one can count four doublets (α, β, γ and δ from lower to higher magnetic field). Cross peaks between α and γ, and between β and δ are detected in COSY spectrum of **1b** at 213K. This means that there are two types of bridging methylene groups in **1b**. Moreover, α and γ can be assigned to axial and equatorial protons in the same methylene groups of one type, respectively. β and δ can be assigned to axial and equatorial protons of the other type, respectively. By changing

the concentration from 0.56 mmol dm^{-3} to 4.42 mmol dm^{-3}, γ and δ which are assigned to equatorial protons do not or only slightly move to lower magnetic field (0.00 and 0.03 ppm, respectively). One of the axial protons β moves to lower magnetic field only by 0.02 ppm whereas the other α moves by 0.17 ppm, changing the peak shape. As shown by Fukazawa *et al.*, [14] the dimerization occurs via the intermolecular hydrogen-bonding interaction between the terminal OH groups and the down-field shift is probably due to the intermolecular shielding effect induced in the dimerization.

Conclusions. Although the computational study assumes the gas phase whereas the ^1H NMR study is carried out in solution, we obtained several correlative findings from the combined studies. i) Molecular mechanics studies suggest that the calix[4]arene framework with no OH group favors a cone conformation with C_4 symmetry and the changes in the relative stabilities in calix[4]arenes with OH-groups are due to the formation of stable hydrogen bonds and/or the relaxation of the steric crowding around OH-substituents in a lower rim site. ii) With depleting OH groups the energy differences between cone conformation and other three conformations becomes smaller. iii) The ROESY spectrum of **2b** at low temperature can be assigned reasonably by assuming a mixture of cone and 1,3-alternate. Moreover, that of **3b** can be assigned as a mixture of two types of interconversion processes: interconversion between cone and partial cone and that between 1,3-alternate and partial cone. iv) VT-NMR studies also show that the ring inversion barriers of calix[4]arenes increase with the number of OH groups in 25, 26, 27 or 28-position. v) The concentration dependence of the NMR spectra suggests that mono-OH-depleted calix[4]arene **1b** forms intra- and intermolecular hydrogen bonds among phenolic OH groups, while di- and tri-OH-depleted calix[4]arenes (**2b** and **3b**) scarcely form it. We believe that these conclusions are useful to understand the influence of OH groups in calix[4]arene homologs.

Acknowledgment. We thank H. Matsumoto for helpful discussions on the 2-D NMR experiment.

Supplementary Material Available. Tables and Figures of MM3(92)-calculated energy terms of all compounds : **0a** ~ **4a**, **0b** ~ **4b** shown in scheme 1 and a Table of MM3(92)-calculated thermodynamic parameters of **0a** ~ **4a**.

References

(1) H. H. Minn, S. K. Chang and K. T. No, *Theor. Chim. Acta*, **75**, 233 (1989).
(2) S. Shinkai, K. Iwamoto, K. Araki and T. Matsuda, *Chem. Lett.*, 1263 (1990).
(3) P. D. J. Grootenhuis, P. A. Kollman, L. C. Groenen, D. N. Reinhandt, G. J. van Hummel, F. Ugozzoli and G. D. Andreetti, *J. Am. Chem. Soc.*, **112**, 4165 (1990).
(4) J. Roger, F. Bayard and C. Decoret, *J. Chim. Phys.*, **87**, 1695 (1990).
(5) S. Miyamoto and P. A. Kollman, *J. Am. Chem. Soc.*, **114**, 3668 (1992).
(6) E. Dohan and S. E. Biali, *J. Org. Chem.*, **56**, 7269 (1991).

(7) C. D. Gutsche, *Acc. Chem. Res.*, **16**, 161 (1983).

(8) C. D. Gutsche, " Calixarenes", Royal Society of Chemistry, Cambridge, 1989.

(9) S. Shinkai, *Bioorg. Chem. Front.*, **1**, 161 (1990); S. Shinkai, *Tetrahedron*, **49**, 8933 (1993).

(10) K. Iwamoto, K. Araki and S. Shinkai, *J. Org. Chem.*, **56**, 4955 (1991).

(11) L. C. Groenen, J.-D. dan Loon, W. Verboom, S. Harkema, A. Casnati, R. Ungaro, A. Pochini, F. Ugozzo and D. N. Reinhaudt, *J. Am. Chem. Soc.*, **113**, 2385 (1991).

(12) T. Harada, J. M. Rudzinski and S. Shinkai, *J. Chem. Soc. Perkin Trans. 2*, 2109 (1992).

(13) T. Harada, J. M. Rudzinski, E. Osawa and S. Shinkai, *Tetrahedron*, **49**, 5941 (1993).

(14) N. L. Allinger, Y. H. Yuh, and J. -H. Lii, *J. Am. Chem. Soc.*, **111**, 8551, 8566, 8576 (1989). The MM3(89) and MM3(92) programs for the UNIX system were obtained from Technical Utilization Corporation, Inc., 235 Glen Village Court, Powell, OH 43065 (U.S.A.). See manual and references cited therein.

(15) F. Grynszpan, Z. Goren and S. E. Biali, *J. Org. Chem.*, **56**, 532 (1991).

(16) Y. Fukazawa, K. Deyama and S. Usui, *Tetrahedron Lett.*, **33**, 5803 (1992).

(17) J. E. McMurry and J. C. Phelan, *Tetrahedron Lett.*, **32**, 5655 (1991).

(18) F. Grynszpan and S. E. Biali, *Tetrahedron Lett.*, **32**, 5155 (1991).

(19) F. Grynszpan and S. E. Biali, *J. Phys. Org. Chem.*, **5**, 155 (1992).

(20) Y. Ting, W. Verboom, L. C. Groenen, J.-D. van Loon and D. N. Reinhoudt, *J. Chem. Soc., Chem. Commun.*, 1432 (1990).

(21) F. Ohseto, H. Murakami, K. Araki and S. Shinkai, *Tetrahedron Lett.*, **33**, 1217 (1992).

(22) U. Burkert and N. L. Allinger, *Molecular Mechanics*, ACS, Washington D.C. (1982).

(23) MOLGRAPH™ is a molecular design support system from DAIKIN Co. Ltd., 1994.

(24) D. S. Stephanson and G. Binsch; modified by C. B. LeMaster, C. L. LeMaster and N. S. True, *QCPE* #569. See manual and references cited therein.

(25) We use a special conformational descriptor for this unique-1,2-alternate structure. We divide the molecule into two parts along the line connecting two opposite methylene carbons so that two of the four phenyl rings can be on the same side of the reference plane. In each substructure the angle between phenyl ring and the plane defined by the three methylene carbon atoms can be directly compared to the angle between the phenyl ring and the reference plane in other structures. See also ref. 13.

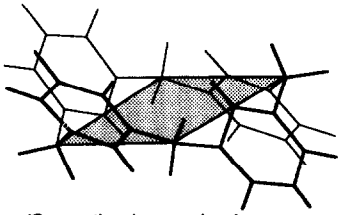

'Conventional mean plane' for typical-1,2-alternates (**0a**, **1a** and **2a**)

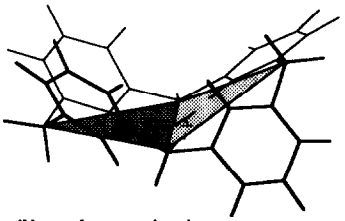

'New reference plane' for unique-1,2-alternates (**2'a**, **3a** and **4a**)

(26) In fact, we recently found ^{1}H NMR spectral evidence that some calix[4]arene-25,26,27,28-tetrols adopt C_2 symmetry: A. Ikeda and S. Shinkai, *J. Chem. Soc., Perkin Trans. 2*, in press.

(27) K. Araki, S. Shinkai and T. Matsuda, *Chem. Lett.*, 581 (1989).

(*Received in Japan* 1 *September* 1994; *accepted* 4 *October* 1994)